Feasibility of an Electrical Interconnect in Carbon-Nanotube-Templated Microfabrication

Berg Dodson

A senior thesis submitted to the faculty of
Brigham Young University
in partial fulfillment of the requirements for the degree of

Bachelor of Science

Richard Vanfleet and Robert Davis, Advisors

Department of Physics and Astronomy

Brigham Young University

April 2017

Copyright © 2017 Berg Dodson

All Rights Reserved

ABSTRACT

Feasibility of an Electrical Interconnect in Carbon-Nanotube-Templated Microfabrication

Berg Dodson
Department of Physics and Astronomy, BYU
Bachelor of Science

Metal electroplating of carbon nanotube (CNT) forests is viable method for fabricating metal microelectromechanical systems (MEMS). Recent work has demonstrated that electroplating an interconnected carbon nanotube structure is possible through direct electrical contact to the CNT structure. However, this is not ideal since features in MEMS fabrication often need to be both electrically and mechanically isolated from each other. Current efforts have been directed toward electroplating CNT patterns through electrical contacts on the substrate. In this case contacting to CNTs through metallic leads that sit between the substrate and the grown CNT forests. Since the CNT forest catalyst layer involves an insulating, alumina diffusion barrier between the iron catalyst layer and the metallic substrate, this is not as simple as it sounds. Results on the measured resistance of this structure are presented in this thesis.

Keywords: Carbon nanotubes, carbon-nanotube-templated microfabrication, resistance, four-point probe, two-point probe

ACKNOWLEDGMENTS

I would like to thank everyone who helped and contribute to the work that went into completing this thesis. Particularly, I would like to thank my advisers, Dr. Richard Vanfleet and Dr. Robert Davis, for their guidance on this project. I would also like to thank Guohai Chen for being the lead researcher on this project and lending some of the images featured in this thesis.

Contents

Table of Contents **iv**

List of Figures **v**

1 Introduction **1**
1.1 Microelectromechanical Systems (MEMS) 1
1.2 Carbon Nanotubes 3
1.3 Objectives of this Project 8

2 Methods and Data **10**
2.1 Sample Preparation 10
2.2 Testing 13
2.3 Pre-Growth Tests 16
2.4 Finished Device Resistance 21

3 Conclusions **25**

Bibliography **27**

List of Tables

2.1 Table comparing the resistances of several tungsten Samples. 19

2.2 Table comparing the resistances of several tungsten Oxide Samples. 19

2.3 Table showing measured resistances for the completed MEMS sensors. 23

List of Figures

1.1 Examples of MEMS 2

1.2 Demonstration of a CNT structure that has been grown to over a millimeter 4

1.3 Examples of CNT structures 5

1.4 Consecutive layers of thin films needed to grow carbon nanotubes 6

1.5 Image of the photolithography mask used to pattern the samples 7

1.6 The stack of thin films that were used to make the MEMS device 9

2.1 Images of the completed samples 12

2.2 Diagrams of the setup for four-point and two-point probe measurements 14

2.3 Qualitative comparison of an oxidized sample and a pure tungsten sample 16

2.4 XEDS spectrum taken on a tungsten oxide sample 17

2.5 The setup used for the four-point probe measurements 18

2.6 A comparison of a representative set of VI graphs taken from measurements made on the tungsten oxide sample 20

2.7 Setup for performing a two-point probe measurements 22

2.8 Figure comparing the VI graphs of the completed MEMS sensors 24

Chapter 1

Introduction

1.1 Microelectromechanical Systems (MEMS)

Microelectromechanical systems (MEMS) are small devices. MEMS are traditionally made with common microfabrication methods such as physical and chemical vapor deposition, wet and dry etching, and photolithography. Using these techniques, MEMS devices can be made to be on the order of 1 to 100 μm in size.

The size of these devices makes them versatile. Airbags, cellphones, thermometers, and video game controllers, and almost all modern devices use MEMS devices. They can perform a variety of functions, but generally their purpose can be described as either that of actuation or sensing.

As an example, a BYU research group under Dr. Brian Jensen recently developed a MEMS device that functions as a DNA injector. It works based on physical actuation. In figure 1.1 the DNA injector is brought up to the egg by inserting tweezers into the large circle on the square portion of the lance and pushing it forward. This allows the device to lift up off the substrate it was made on and inject the DNA on its tip into the egg. It is through actuation in this case that the device accomplishes its goal.

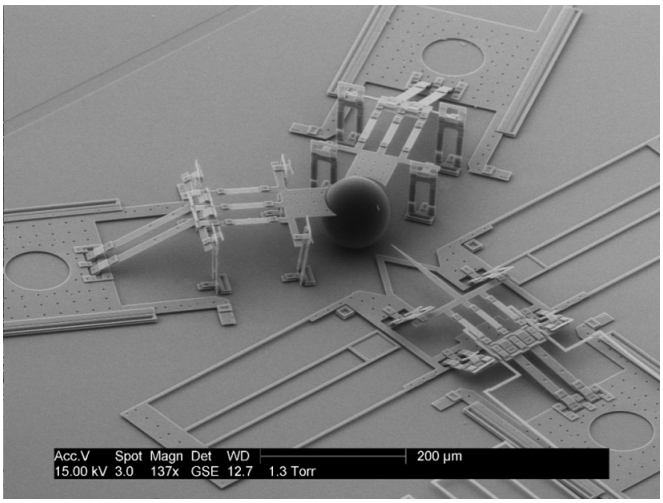
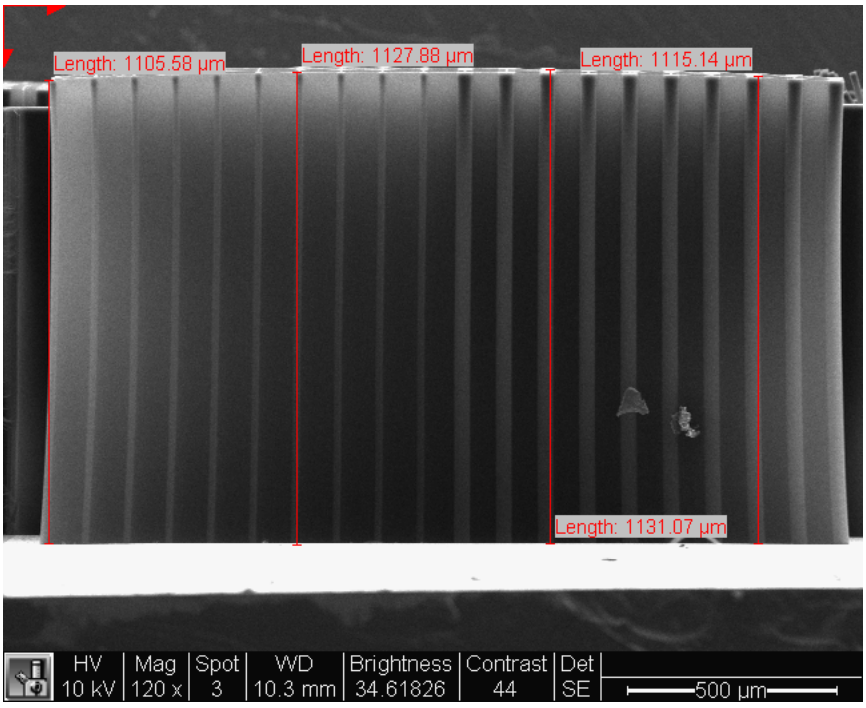


Figure 1.1 MEMS, micro-devices, are able to perform tasks on the micro-scale. Here is a MEMS device that, when pushed, actuates and folds up, forcing a DNA lance, the needle portion, into a mammalian egg, represented by the silica bead. Credit to Dr. Jensen for the image.

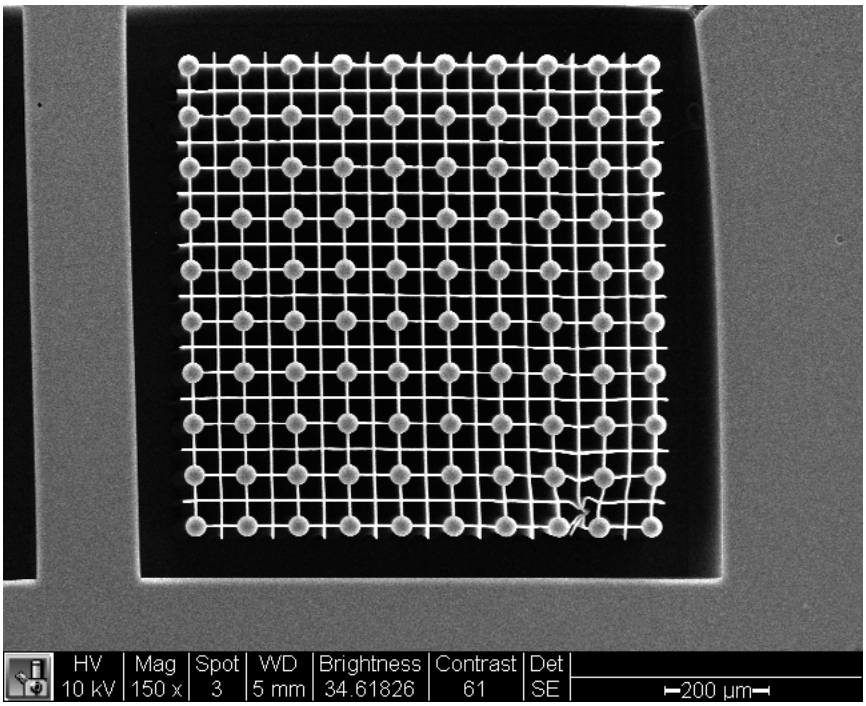
This device highlights some of the difficulties of making MEMS. In order to function, part of the machine's actuation includes lifting up the DNA lance so it can penetrate the egg. This lack of a three-dimensional form is not unique to this device, but is common to almost all MEMS devices: they are practically two-dimensional devices. The reasons MEMS are essentially two-dimensional is a function of the fabrication process where slow etch rates and thin film stresses limit devices' thickness. Slow etch rates are essential for control of how much material is removed in an etch, but they limit depth and undercut times that can be sustained in a commercial process. When depositing material on the substrate it is nanometer by nanometer. For depositions that are only a few nanometers this isn't a problem, but internal stress builds up as the deposition becomes thicker. If the internal stress is large enough, this will cause the device to curl up off the substrate, usually ruining the device. Thus, deposits are limited to quasi-two-dimensional patterns.

1.2 Carbon Nanotubes

One material that may be able to help make taller MEMS is carbon nanotubes (CNTs), see figure 1.3. A carbon nanotube, simply described, is a form of carbon where all the atoms have bonded in the shape of a tube. These CNTs form in such a way that their cross section is only a couple of nanometers in diameter, but their height can reach beyond a millimeter, as in figure 1.2.



(a)



(b)

Figure 1.2 Image of a CNT MEMS device that has been grown to over a millimeter tall. In image (a) we can see that the structure has been grown to over 1.1 millimeters tall. In image (b) we can see that the CNT forest has been patterned to make an array of CNT posts with interconnecting hedges.

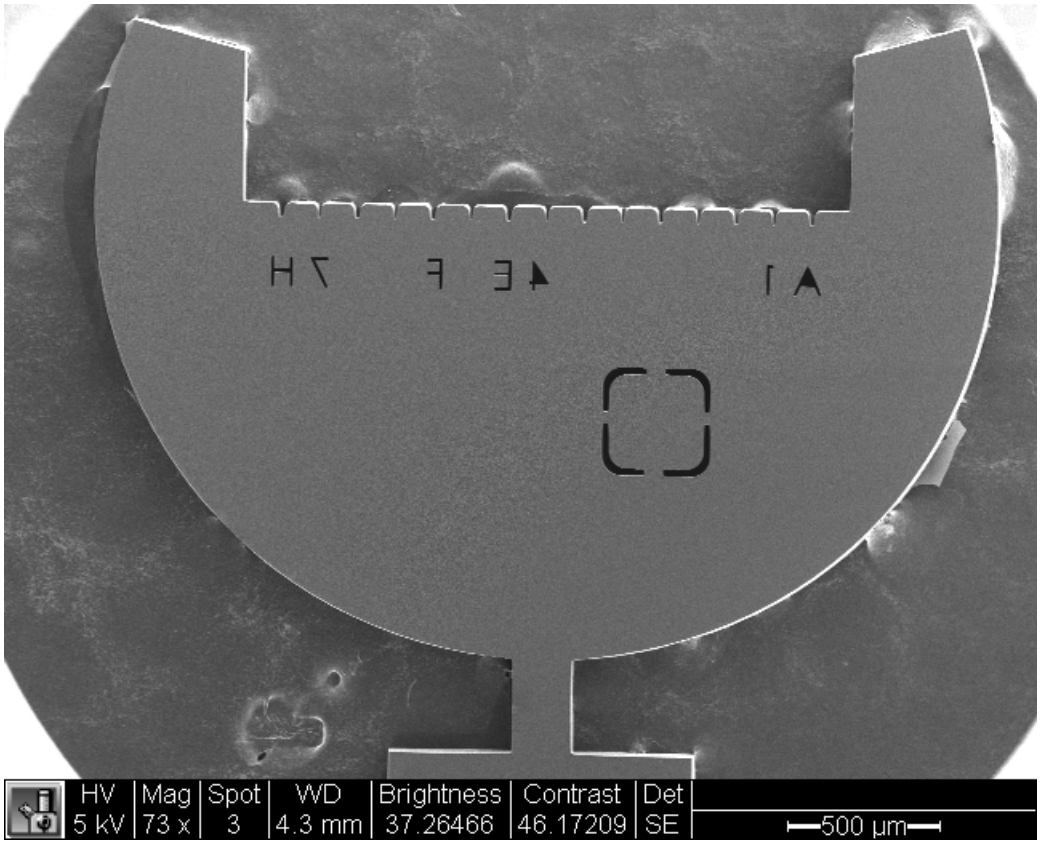


Figure 1.3 An example of a MEMS device, a TEM grid, made of CNTs. This device was made by growing CNTs and then infiltrating them with carbon.

In addition to having a high aspect ratio, CNTs also possess a large tensile strength [5] and are electrically conductive.

Standard CNT forest growth requires a substrate material, usually a silicon wafer, and a few thin film layers. The first step is depositing a layer of alumina on top of the substrate using electron beam physical vapor deposition (PVD). This layer acts as a diffusion barrier which will help keep the iron deposited on top of it from diffusing into the silicon wafer below as well as impact the horizontal diffusion of the iron [1]. After the diffusion barrier has been put down, iron, the catalyst for CNT growth, is deposited on the wafer through thermal evaporation. Finally, the sample is then put in a furnace for chemical vapor deposition (CVD) growth of the CNTs, as shown in figure 1.4.

This type of growth results in CNTs growing in a large group across the wafer, a "forest" of

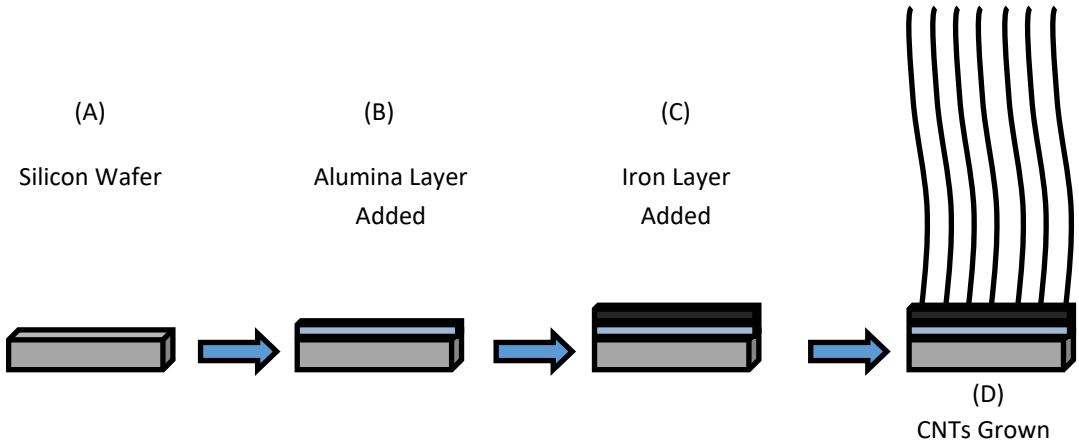


Figure 1.4 In order to grow carbon nanotubes, several thin films need to be deposited on top of (A) a silicon wafer. The first is (B) alumina which is deposited by electron beam physical vapor deposition. The second, (C), is iron which is deposited by thermal evaporation. Carbon nanotubes (D) are finally grown through chemical vapor deposition.

CNTs. Patterning the CNT forest is required to make a MEMS device.

The first step in patterning a CNT MEMS device involves restricting where the iron is deposited. This is done using a technique called photolithography. It works by applying a chemical called photoresist onto the wafer. Photoresist breaks down and becomes soluble in a developer solution once it is exposed to uv light. The two chemicals, the photoresist and the developer, are AZ3330 and 300 MIF, respectively. A patterned light "mask," see figure 1.5, exposes the areas where CNTs need to grow to uv light. The pattern on the mask is transferred onto the wafer by developing the wafer, putting it in a 300 MIF bath, once the wafer has been exposed.

The photoresist that is left on the wafer shields those regions during subsequent material depositions. The pattern in figure 1.5 is used for alumina and iron depositions. After the alumina and iron have been deposited, the remaining photoresist is removed with 1-Methyl-2-pyrrolidinone (NMP). The NMP removes the AZ3330 along with the material that has been deposited on top of it. This means that the regions where photoresist was initially removed are the only regions where alumina and iron are left. Consequently, CNTs will only grow in these regions since they are the

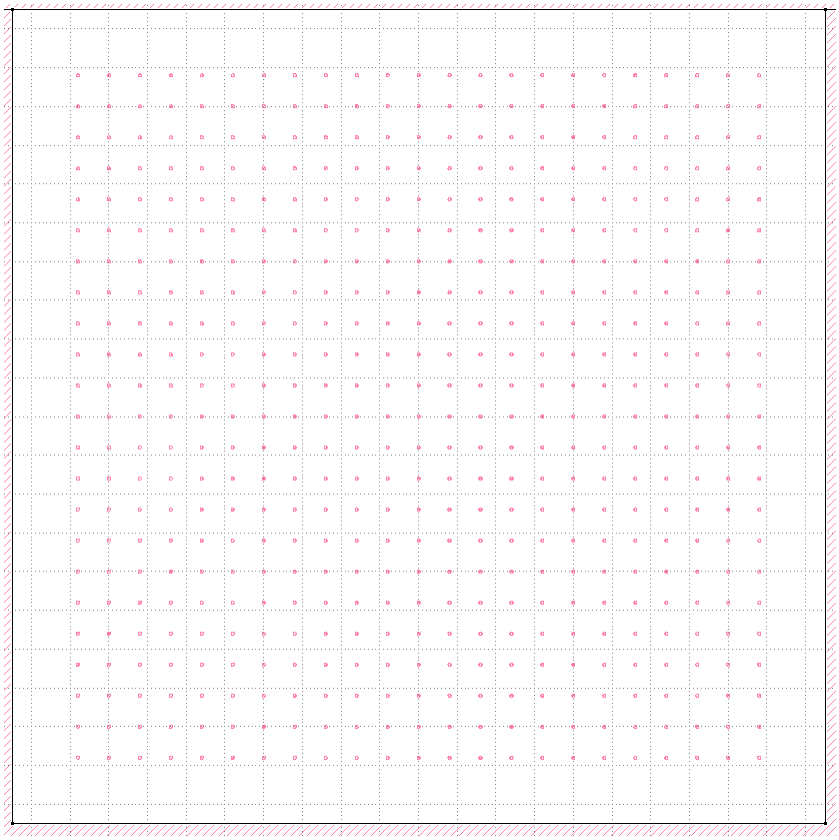


Figure 1.5 A magnified image of the pattern that was used for the alumina and iron photolithography mask. The areas that are marked in dashed pink lines are the area where uv light was allowed to hit the AZ3330 on the wafer. All other areas were protected from the uv light.

only areas with iron on the wafer [2]. By controlling where the iron is deposited on the wafer, a projection of the MEMS we want to make can then be extruded from the pattern of iron by growing CNTs.

Once the CNTs have been patterned and grown, they can serve as a scaffold for the MEMS device. This scaffold can be infiltrated with other material using CVD, PVD, electroplating, or any other method for for depositing a material [3–5]. Since the volume occupied by a CNT forest is only composed of about one percent CNTs by volume, there is a lot of empty space. This is filled in by an infiltrating material. The infiltrated CNT forest has increased strength and the desired material properties [5].

1.3 Objectives of this Project

The objective of this project is test the feasibility of using Carbon-nanotube-templated microfabrication (CNT-M) to make a sensor composed of an array of CNT posts with indirect electrical contacts to the CNT posts. We first put down a layer of tungsten on the silicon wafer before depositing the normal layers of alumina and iron, as depicted in figure 1.6. The tungsten layer serves as a conductive base to connect to the CNTs device. The question of whether or not CNTs can grow with a metallic layer beneath them has been addressed previously [6–9]. In particular, we tested to see whether or not an electric current could pass through the metallic and alumina layers and move through the CNTs. Even though CNTs are conductive the alumina diffusion barrier is an insulator and may prevent current flow between the CNTs and metallic thin film layer. Unfortunately, alumina is essential for CNT forest growth and cannot simply be discarded. Fortunately, the thickness of the alumina layer is no more than 40 nm, and as resistance is proportional to thickness, it is possible that the alumina layer will not have a large resistance.

The following chapters will describe how the samples were prepared for testing, the manner in

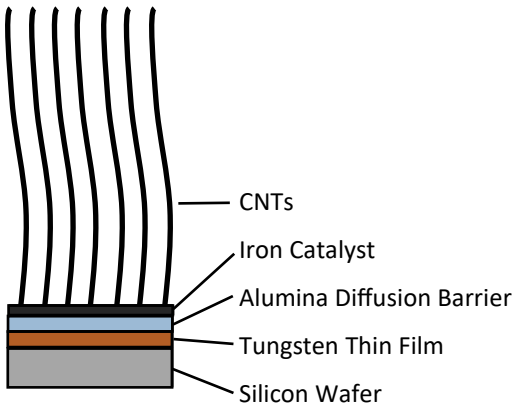


Figure 1.6 Several thin films were deposited on top of the silicon wafer to make the MEMS sensor device. Tungsten, alumina, and iron were deposited on the wafer in that order before carbon nanotubes were grown.

which the tests were conducted, and finally the results of the conductivity measurements.

Chapter 2

Methods and Data

In this chapter the preparation taken to conduct the resistance measurements of the samples will be discussed. This discussion begins with an overview of sample preparation. The various deposition methods and the order they are performed in are noted. Subsequent tests that were performed to standardize and control the quality of the samples are also explained. A review of the setup for the actual resistance measurements at various stages of the project is given and explained. Finally, the resistances of the samples at different stages of the project are given.

2.1 Sample Preparation

Before growing CNTs, several thin films must be deposited on a silicon wafer. This stack of thin films can be divided according to the purpose they serve. The three different layers are the substrate, the diffusion barrier, and the catalyst layer on top of which the CNTs are grown.

The substrate is the conductive, metallic layer through which the electric current flows and is deposited first. Previous work done by Marcus Finlinson demonstrated that the material and thickness of this layer affects the growth rate of the carbon nanotubes [10]. The results indicated that tungsten gave consistent growth rates and had similar growth to normal CNT growth on a

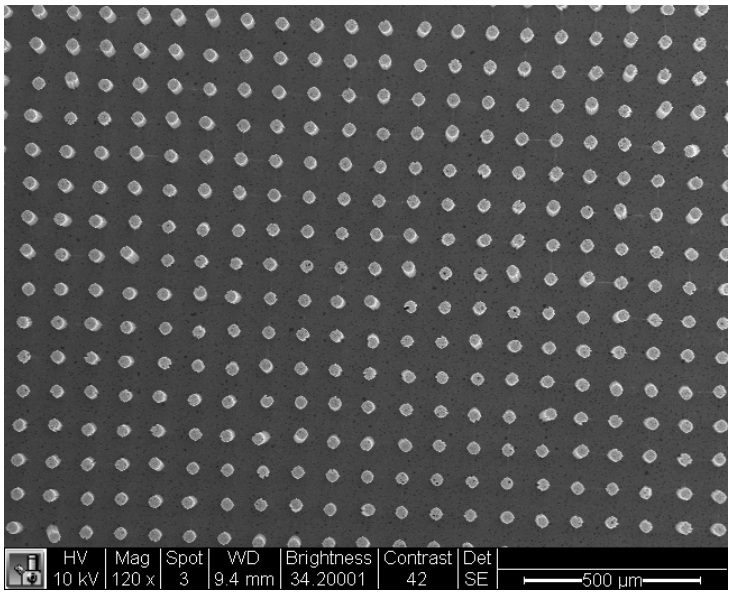
silicon substrate. This makes it suitable for being used as the conductive layer and, thus, was chosen.

The diffusion barrier is the second thin film to be deposited and is used to keep the catalyst layer from diffusing into the underlying layers of the stack. If this layer is not present the iron catalyst will diffuse into the underlying material and no CNT growth occurs [1].

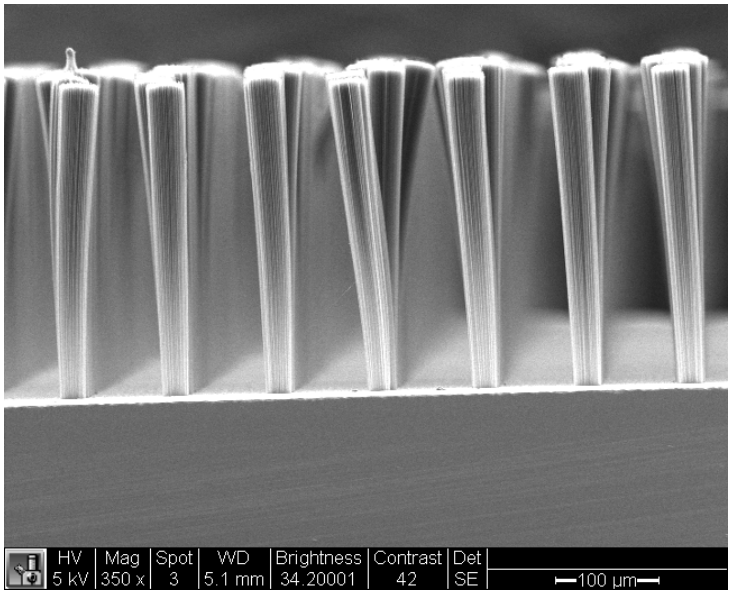
On top of the diffusion barrier is the catalyst layer which facilitates CNT growth during CVD. The thickness of this layer also affects how tall the CNTs will grow. For our research group's equipment, the tallest and most consistent growths have been observed while using 4 nm of iron. Since the MEMS sensor needs to have a high aspect ratio, this thickness was used to promote the tallest achievable growth.

The steps to create the CNT structures are standard procedures and are the same as the procedures that are used by Dallin Barton [3], Lawrence Barrett [12], and others in the Davis research group [4]. These steps will not be treated in depth in this thesis, but simply listed. The steps are:

1. 100 nm of tungsten are deposited via sputtering.
2. Photolithography is performed. The pattern used during this step is the same as the one depicted in 1.5.
3. 40 nm of alumina are deposited via electron beam deposition.
4. 4 nm of iron are deposited via thermal evaporation.
5. A protective layer of photoresist is deposited and the wafer is diced into individual samples using the dicing saw.
6. The photoresist is removed in a 15 minute NMP bath.
7. Carbon nanotubes are grown via chemical vapor deposition.



(a)



(b)

Figure 2.1 Images taken of the completed samples with a top down view seen in (a) and a side view of the sample seen in (b). The sensor is composed of several CNT posts all of which are lined up in a nice array.

2.2 Testing

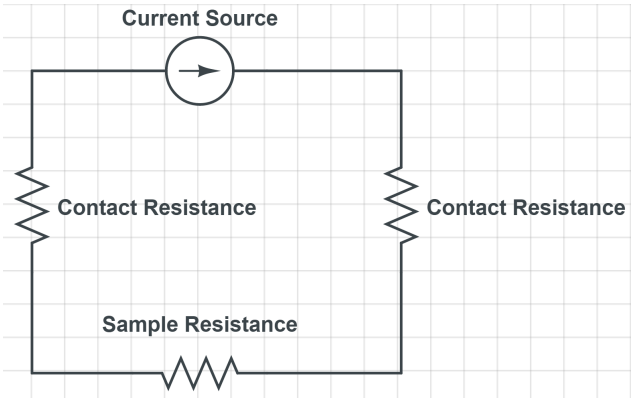
Many tests were performed on the samples during the project. These test verified that the correct material had been deposited during a deposition or gave us data about the resistance of the MEMS device at different stages of fabrication.

X-ray energy dispersive spectroscopy (XEDS) was one of the tests performed on the samples and was used to determine their chemical composition. To perform XEDS, the sample is placed in a scanning electron microscope (SEM) and bombarded with a beam of energetic electrons. These beam electrons ionize the atoms in the sample by ejecting an inner shell electron. The ionized atom subsequently relaxes from its ionized, high-energy state when an outer shell electron drops down and occupies the inner shell site. This relaxation emits a characteristic x-ray which is collected by a detector in the microscope. By observing the characteristic x-rays that are collected, the chemical constituents of the sample can be determined. In this way, we can determine the chemical makeup of the sample and see if there are contaminants in the sample.

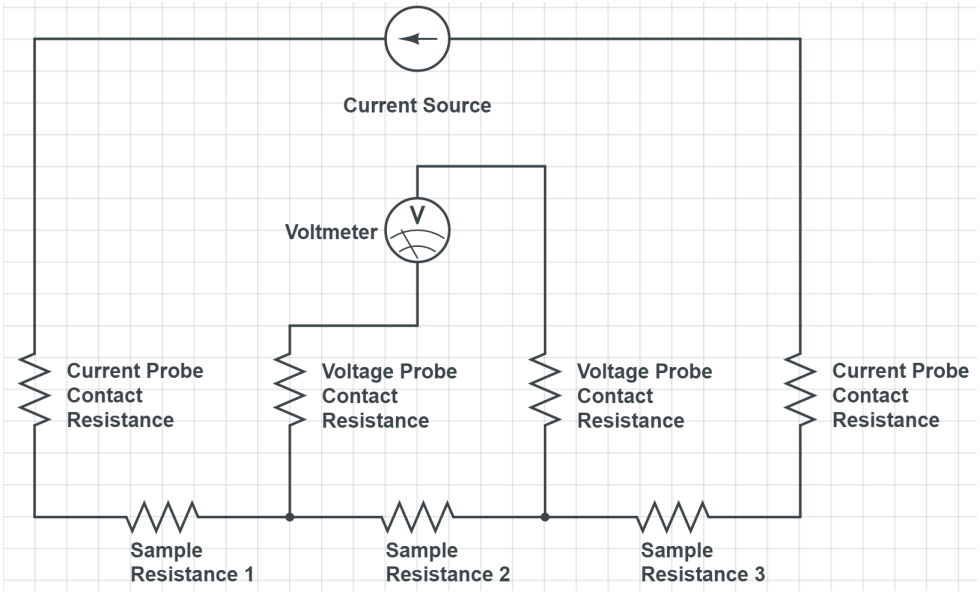
This test cannot conclusively answer whether or not there is sample contamination, though, but rather serves as an indicator of whether more tests need to be carried out. This is because the electron beam ionizes atoms throughout its interaction volume, the volume within the sample that beam electrons travel through before losing all their energy. The size of the interaction volume is on the order of microns while the thickness of the thin films we want to analyze is on the order of nanometers. This means, inevitably, many of the x-rays collected by the detector will come from outside the thin film we're analyzing, and may include characteristic x-rays from other regions of the sample. Thus, additional tests were always performed in conjunction with XEDS.

To test resistance of the MEMS device, four-point and two-point probe measurements were performed, see figure 2.2. These measurements can help determine the conductivity of thin films that have been deposited or, ultimately, help determine the resistance of the completed samples.

Two-point probe measurements were performed by attaching the two leads of an ohmmeter to



(a)



(b)

Figure 2.2 Diagrams of where the resistance is in two-point and four-point probe measurements. In a two-point probe measurement, the potential difference is read on either side of the current supply. In the four-point probe method, the potential difference is read across a section of the sample. However, since there is no current flowing through the voltmeter, only the potential difference is only a measure of the samples resistance and not the contact resistances.

the sample and measuring the equivalent resistance between the two probes. This is a quick and simple test to determine whether or not a material is conductive or insulating and helps to quickly distinguish between tungsten and tungsten oxide. The inherent problem with performing two-point probe measurements is that there will be a contact resistance introduced into the measurement just as a result of placing the probes on the sample. Thus the measured resistance, in the case shown in figure 2.2.a will be the sum of the actual resistance and the two contact resistances. In other words, $R_{measured} = R_{sample} + R_{contact1} + R_{contact2}$. This causes resistance readings to be skewed by an unknown and potentially large amount. Fortunately, four-point probe measurements can overcome this inadequacy.

The four-point probe measurement, diagramed in figure 2.2.b utilizes four probes, two of which pass current through the sample and two more probes which measure the relative voltage difference between them. The benefit of this method is that no current flows through the probes that are measuring the voltage and thus remove their contribution to the measured resistance. In this case only the resistance from the sample is measured and so $R_{measured} = V/I = R_{sample}$. An additional benefit is that the four-point probe method can be extended to any two-dimensional sample and allows us to calculate the resistivity of the sample as well [13].

These two methods were used at different times during the project. While the samples were flat, i.e. before growing CNTs, the four-point probe method was employed. However, once CNTs were grown, the sample no longer possessed a flat surface that could accommodate all four probes. This meant that a four-point probe measurement could no longer be used; the two-point probe measurement, despite its shortcomings, was used as an alternative. However, the previous four-point probe measurements done on each of the thin film layers can aid in determining the layers' approximate resistivity and consequently what portion of the final resistance each thin film is responsible for. From these calculations, the approximate resistance and resistivity of the CNTs can be calculated once the two-point probe measurements have been completed.

2.3 Pre-Growth Tests

While making the samples, the tests described in section 2.2 were performed on the samples when we obtained two wafers that had very different appearances, see figure 2.3. Both wafers had been sputtered for the same amount of time, but visually appeared different. First XEDS was performed followed by four-point probe tests.

When the sample was put in the SEM, the spectrum in figure 2.4 was obtained. There is an obvious tungsten peak at 1.775 keV and the silicon peak that would be at 1.740 keV forms the shoulder on left side of the tungsten peak. These are two peaks that we would expect from a normal tungsten sample. However, in addition to the tungsten and silicon peaks, there is also a significant oxygen peak in the spectrum around 0.525 keV. Seeing this oxygen peak means that



(a) **(b)**

Figure 2.3 Both of these wafers have just been sputtered with what should be 100 nm of tungsten. The wafer in (a) has 100 nm of tungsten, but the wafer in (b) has 100 nm of tungsten oxide, turning what should be a conductive silvery layer tungsten into a nonconductive brown tungsten oxide.

there is oxygen in the sample and possibly that it is in the form of tungsten oxide.

The presence of an oxygen peak does mean there is tungsten oxide in the sample, though, and there are a couple of alternate explanations. The oxygen peak in the spectrum only means that there is oxygen somewhere in the interaction volume. Since the interaction volume can be a few hundred nanometers deep, this well exceeds the thickness of just the tungsten thin film and will include some of the silicon wafer as well. Silicon wafers generally have a silicon oxide film on their surface. This oxide layer, since it is part of the interaction volume, could be contributing some, if not all, of the oxygen peak counts. Due to this complication, it was impossible to say definitively whether or not the sample included tungsten oxide.

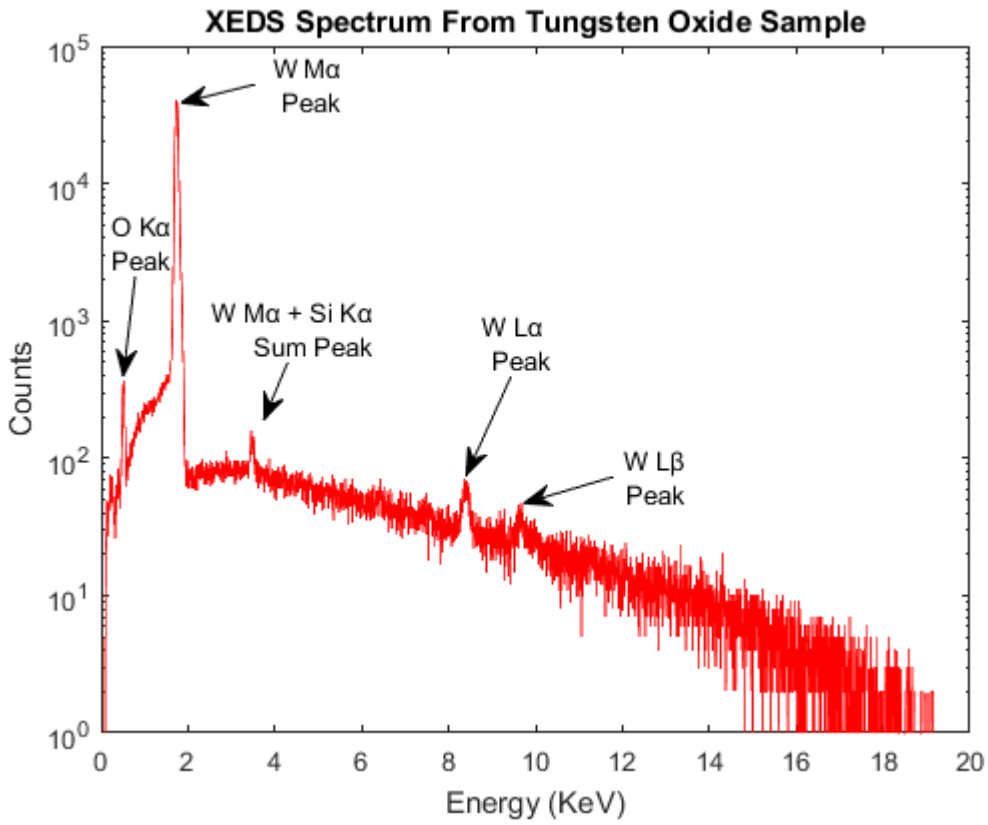


Figure 2.4 This is the XEDS spectrum that was obtained from a tungsten oxide sample. There is an obvious tungsten peak at 1.775 keV and an obvious oxygen peak around 0.525 keV which indicates that there is oxygen in the sample and suggests the presence of tungsten oxide.



Figure 2.5 Four probes are used in four point probe measurements, two probes on to each layer of the sample. Of the two probes on each layer, one provides current for the measurement and the other measures the voltage.

To determine if the oxygen was from tungsten oxide, the electrical resistance of the sample was measured using four-point probe measurements to see if the resistance corresponded better to tungsten or tungsten oxide. The thought was that the tungsten samples should have a significantly lower resistance than a tungsten oxide sample. Measurements performed on the samples similar to figure 2.3.a can be found in table 2.1 while the resistance from samples similar to those found in figure 2.3.b yielded the resistances found in table 2.2.

Resistances of Tungsten Samples	
Sample	Resistance (Ω)
Sample 1	93.2
Sample 2	92.3
Sample 3	103.2
Sample 4	84.5

Table 2.1 Table displaying the resistances that were measured on the tungsten samples. These measurements were made using the four-point probe method. While the measurements of the resistance vary slightly, this can be attributed to slight changes in the geometry of the probes since they varied slightly between samples. These resistances are fairly consistent though between measurements and between samples.

Resistances of Tungsten Oxide Samples	
Sample	Resistance (GΩ)
Sample 1	0.0108
Sample 2	0.115
Sample 3	1.11
Sample 4	7.30
Sample 5	30.6

Table 2.2 Table displaying the resistances that were measured on the tungsten oxide samples. These measurements were made using the four-point probe method. While the resistances seem high, it is likely a result of the current meter not being sensitive enough to detect any current that was in the samples and only reporting noise. The take away is that the tungsten oxide samples are non-conductive.

The resistances measured from the many of the samples with a silver colored thin film had low resistances, most below 100 Ω, which was consistent with what was expected after a tungsten deposition. The samples that looked more like those in figure 2.3.b had resistances which were

incredibly high, they are most likely not accurate. The VI graphs in figure 2.6 indicate that the measured current was noisy and even included negative values for the current. This is likely not due to the actual current being noisy since our current source is capable of maintaining a stable current, but is more likely due to the ammeter being unable to detect anything above the noise level.

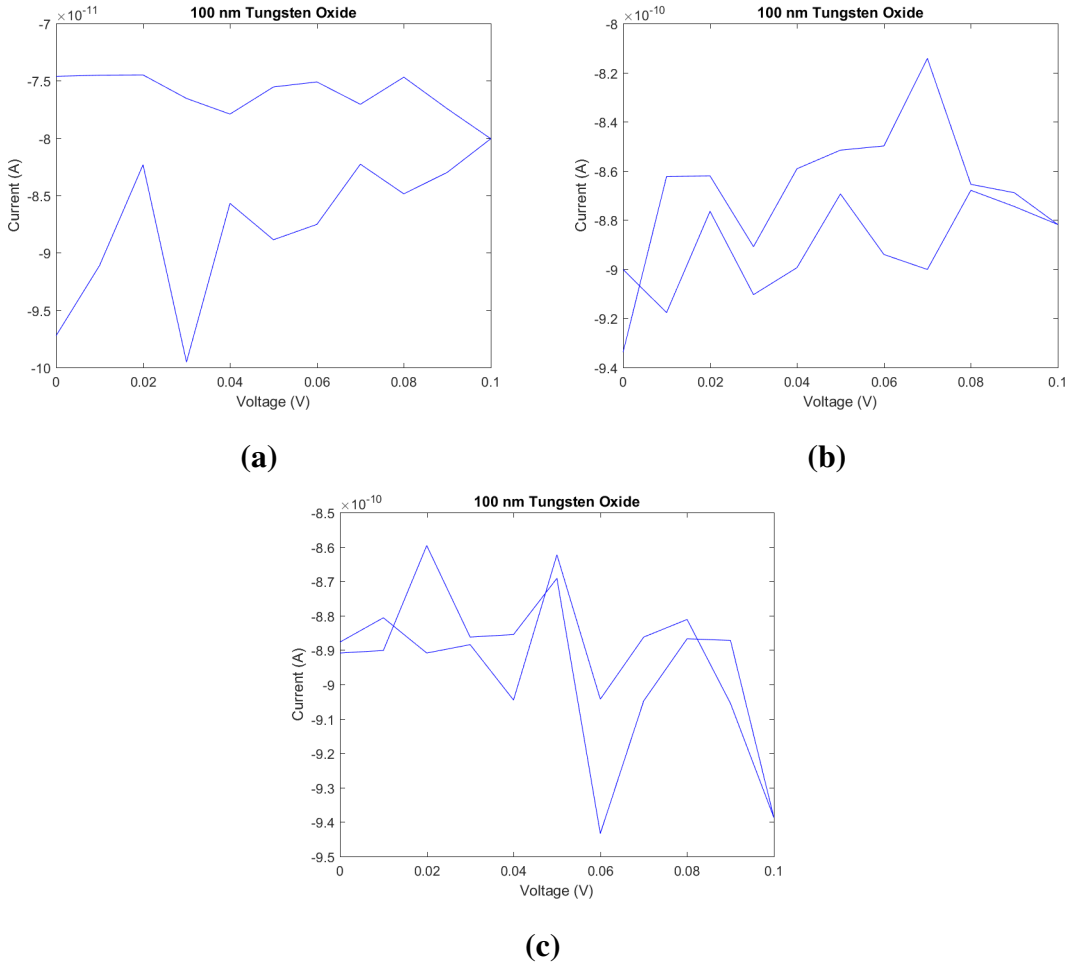


Figure 2.6 Graphs (a), (b), and (c) were all constructed from measurements made on tungsten oxide samples. The graphs are representative in demonstrating what the measurements showed: there was a lot of noise in the measurements and the quite often showed non-sense measurements.

However, since the measured current was so volatile, the resistance for these samples was

obtained by dividing the highest value of the current by the maximum voltage that was applied to the sample. While this gives us values that are to be treated suspiciously, the take away is that the tungsten oxide samples are non-conductive. In order to avoid using oxidized samples, any tungsten deposited wafer that yielded a resistance that was greater than 110 Ω was considered oxidized and discarded.

2.4 Finished Device Resistance

Culminating all of the tests and procedures were the resistance measurements of the completed device. Unlike the previous resistance measurements on the tungsten layer, these measurements answer the overarching question of the entire project: "is this MEMS device conductive?"

In order to perform these measurements, two-point probe measurements were performed instead of four-point probe measurements for the reasons discussed in chapter 2, principally, the dimensions of the CNT posts on the device would not accommodate more than one probe at a time on top of them.

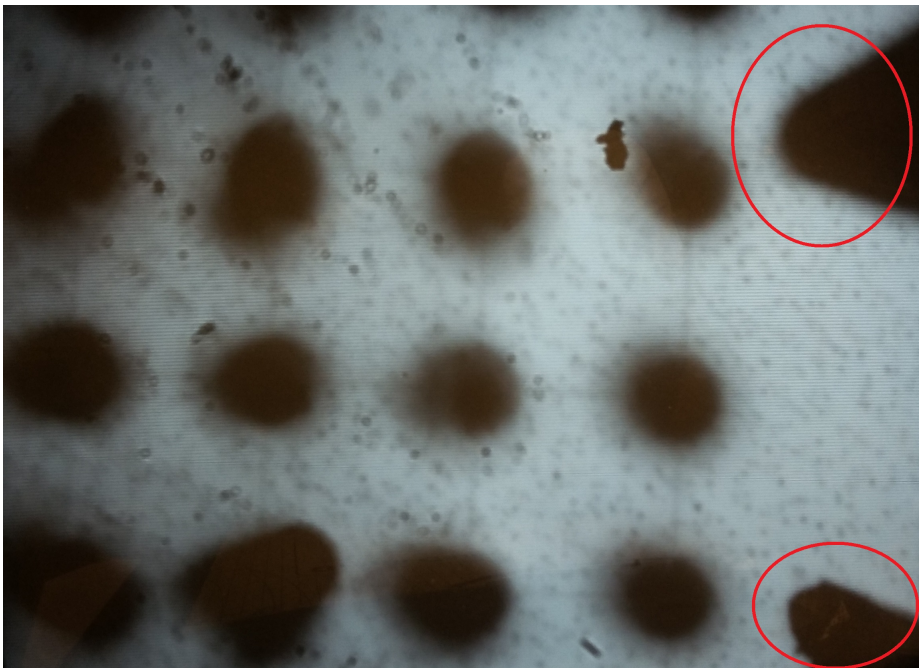


Figure 2.7 This is an image of the posts of the MEMS sensor just prior to performing a two-point probe measurement. The two red circles indicate the position of the probes that will perform the measurement. The size of the probes greatly exceeds the size of a CNT post meaning that only one post will fit onto a CNT post. This made it necessary to use two-point probe measurements.

The implications of this is that there are now two more potential sources of resistance in the structure due to the contact resistance of the probes contacting the tungsten substrate and the CNT posts. This means that the actual resistance of the device should be less than the value that we measure.

The measurements were taken by placing one of the probes on an exposed area of tungsten and placing the second probe on top of a single CNT post. The tungsten probe was lowered until it was seen moving across the surface of the tungsten to ensure it had good contact; the CNT probe was lowered until the CNT post started to bend under the pressure of the probe. Several measurements from several posts were taken to demonstrate reproducibility. Some representative data from those measurements is shown in table 2.3

Resistances of the MEMS Sensor	
Sample	Resistance (Ω)
Sample 1	489
Sample 2	326
Sample 3	355

Table 2.3 Table of a representative set of resistances gathered from making two-point probe measurements on the completed MEMS sensors. The resistances in the hundreds of ohms, meaning they are conductive enough.

The resistance measurements have values that are in the hundreds of ohms. This is low enough to consider them conductive for our application. Not only are the devices conductive, but the response they exhibited an ohmic response during the measurement which can be seen in figure 2.8.

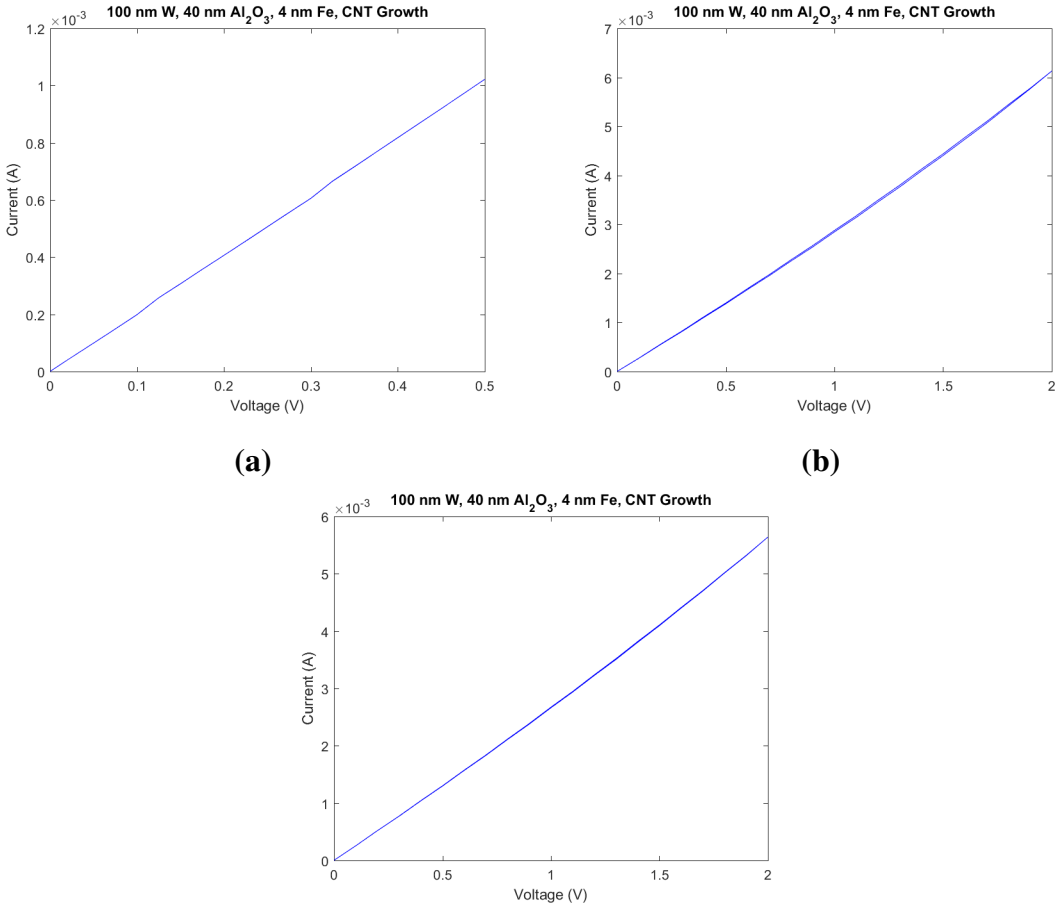


Figure 2.8 Figure comparing the electric responses of the completed probe arrays. Figures (a), (b), and (c) show the VI responses observed while performing the two-point probe measurments on the completed MEMS sensors. The graphs all have a definite linear character which indicates that the samples behave ohmically.

Chapter 3

Conclusions

After measuring the resistances of the completed samples, we were able to see that they were conductive. This is in spite of the alumina diffusion barrier.

The range of resistances given in table 2.3 indicate that the sample is conductive. It also behaves in an ohmic manner, as seen in figure 2.8. This demonstrates that even with the alumina layer between the tungsten and the carbon nanotubes, the device is still conductive. This is surprising since alumina, in bulk has a very high resistivity.

One plausible explanation for the device being conductive in spite of having the alumina layer is that, even though it is a diffusion barrier, some of the iron is diffusing down into it. With this diffusion, it could cause the alumina layer to become more conductive and lower the resistance. It is also possible that the tungsten is diffusing into the alumina layer, and in a similar fashion reducing the resistance of the alumina layer, although this seems less likely since tungsten is less mobile than iron at the temperatures used in the fabrication process.

Now that it has been shown that the completed MEMS sensor is conductive, there are some more things that need to be done to finish the MEMS sensor. The next step will be to create individual tungsten strips that connect to each CNT post in the sensor. This step will allow us to treat each CNT post separately and have give us more resolution when the sensor is finished. An-

other step is to determine whether or not the CNT posts on the sensor can be electroplated without touching them directly. The reason for this is that while the CNT posts serve as a convenient scaffold, they are not strong enough to survive electroplating as it has been done traditionally in our group [4]. However, if we can demonstrate that we can electroplate the posts by connecting an electrode to the tungsten, instead of to the CNT forest, it will be possible to electroplate the sensor without damaging the probes.

Bibliography

[1] B. Yao, R. V. Petrova, R. R. Vanfleet, and K. R. Coffey, "Compositional Stability of FePt Nanoparticles on SiO2gf/Si During Annealing," Journal of Applied Physics 99 (2006).

[2] D. N. Hutchison, N. B. Morrill, Q. Aten, B. W. Turner, B. D. Jensen, L. L. Howell, R. R. Vanfleet, and R. C. Davis, "Carbon Nanotubes as a Framework for High-Aspect-Ratio MEMS Fabrication," Journal of Microelectromechanical Systems **19,** 75 (2010).

[3] D. Barton, "Nickel and Copper Electroplating of Patterned Carbon-Coated Carbon Nanotube Forests for Application ins Microelectricalmechanical Systems and Through-Silicon Vias," Senior thesis (Brigham Young University, Provo, UT, 2014).

[4] L. Barrett, "High-Aspect-Ratio Metal Microfabrication by Nickel Electroplating of Patterned Carbon Nanotube Forests," Journal of Microelectricalmechanical Systems (2015).

[5] B. H. Hanna, W. C. Fazio, J. D. Tanner, J. M. Lund, T. S. Wood, R. C. Davis, R. R. Vanfleet, and B. D. Jensen, "Mechanical Property Measurment of Carbon Infiltrated Carbon Nanotube Structures for Compliant Micromechanisms," Journal of Microelectromechanical Systems **23,** 1330–1339 (2014).

[6] S. Talapatra, S. Kar, S. K. Pal, R. Vajtai, L. Ci, P. Victor, M. M. Shaijumno, S. Kaur, O. Nalamasu, and P. M. Ajayan, "Direct Growth of Aligned Carbon Nanotubes on Bluk Metals," Nature Nanotechnology **1,** 112–116 (2006).

[7] G. Li, S. Chakrabarti, M. Schulz, and V. Shanov, "Growth of Aligned Multiwalled Carbon Nanotubes on Bulk Copper Substrates by Chemical Vapor Deposition," Journal of Materials Research **24,** 2813–2820 (2009).

[8] C. Masarapu and B. a. Wei, "Direct Growth of Aligned Multiwalled Carbon Nanotubes on treated Stainless Steel Substrates," Langmuir **23,** 9046–9049 (2007).

[9] P. M. Parthangal, R. E. Cavicchi, and M. R. Zachariah, "A Generic Process of Growing Aligned Carbon Nanotube Arrays on Metals and Metal Alloys," Nanotechnology **18,** 1–5 (2007).

[10] M. Finlinson, work done on CNT growth when it's grown with 100 nm of various metals underneath the alumina layer. (unpublished).

[11] G. Chen, "Fe thickness,", Email, 2017, this was the email I received from Guohai Chen explaining why we used the various thicknesses of iron and alumina for the MEMS sensor.

[12] L. K. Barrett, "Silicon Carbon Nanotube Lithium Ion Batteries," Masters thesis (Brigham Young University, Provo, UT, 2015).

[13] L. J. van der Pauw, "A Method of Measuring Specific Resistivity and Hall Effect of Discs of Arbitrary Shape," Philips Research Reports **13,** 1–9 (1958).

Index

Alumina, 5, 6, 8, 11

Carbon nanotubes, ii, 3, 5, 6, 8, 10, 11, 15, 21, 22

Photolithography, 11

photolithography, 6

Sputtering, 11

Tungsten, 11, 15, 16, 22